Water Research 115 (2017) 229–235

Contents lists available at ScienceDirect

Water Research

journal homepage: www.elsevier.com/locate/watres

Quantifying tropical peatland dissolved organic carbon (DOC) using UV-visible spectroscopy

Sarah Cook [a, *], Mike Peacock [b], Chris D. Evans [c], Susan E. Page [a], Mick J. Whelan [a], Vincent Gauci [b], Lip Khoon Kho [d]

[a] Centre for Landscape & Climate Research, University of Leicester, Geography, Leicester, LE1 7RH, UK
[b] The Open University, Dept. of Environment, Earth and Ecosystems, Milton Keynes, MK7 6AA, UK
[c] Environment Centre Wales, Centre for Ecology and Hydrology, Bangor, LL57 2UW, UK
[d] Tropical Peat Research Institute, Biological Research Division, Malaysian Palm Oil Board, Bandar Baru Bangi, 43000, Kajang, Selangor, Malaysia

ARTICLE INFO

Article history:
Received 2 December 2016
Received in revised form
24 February 2017
Accepted 25 February 2017
Available online 27 February 2017

Keywords:
DOC
Tropical peat
Water samples
Spectrophotometry
Sarawak

ABSTRACT

UV–visible spectroscopy has been shown to be a useful technique for determining dissolved organic carbon (DOC) concentrations. However, at present we are unaware of any studies in the literature that have investigated the suitability of this approach for tropical DOC water samples from any tropical peatlands, although some work has been performed in other tropical environments. We used water samples from two oil palm estates in Sarawak, Malaysia to: i) investigate the suitability of both single and two-wavelength proxies for tropical DOC determination; ii) develop a calibration dataset and set of parameters to calculate DOC concentrations indirectly; iii) provide tropical researchers with guidance on the best spectrophotometric approaches to use in future analyses of DOC. Both single and two-wavelength model approaches performed well with no one model significantly outperforming the other. The predictive ability of the models suggests that UV–visible spectroscopy is both a viable and low cost method for rapidly analyzing DOC in water samples immediately post-collection, which can be important when working at remote field sites with access to only basic laboratory facilities.

1. Introduction

Dissolved organic carbon (DOC) is derived from the solubilisation of organic matter, and can be leached from the terrestrial landscape into freshwater ecosystems (Thurman, 1985). It plays a crucial role in peatland carbon budgets (Cole et al., 2007; Hulatt et al., 2014; Abrams et al., 2015; Muller et al., 2015) because it represents a carbon loss from the peat itself and, once in the aquatic system can be degraded, both biologically and photo-chemically, liberating CO_2 (carbon dioxide), CH_4 (methane) and CO (carbon monoxide) into the atmosphere (Cole et al., 2007; Clark et al., 2010; Fellman et al., 2014).

Interest in DOC losses from tropical peatlands has increased in recent years, fuelled in part by the realization of how vulnerable this carbon loss pathway is to land-use related disturbance (Moore et al., 2011, 2013; Evans et al., 2014; Rixen et al., 2016). Furthermore, the controls governing DOC mobility and export, along with their wider local and international implications, in the context of the global carbon cycle, still remain uncertain (Evans et al., 2012, 2014).

Measuring DOC directly in the laboratory requires specialised analytical equipment (e.g. a TOC analyser), which may hinder researchers with limited funds and laboratory equipment or those working in remote locations. An alternative and cheaper method is UV–visible spectrometry and spectroscopy, which relies on establishing relationships between DOC quantity and quality (Weishaar et al., 2003), and absorbance values and ratios (Peuravuori and Pihlaja, 1997), along with the ability to derive DOC compositional information based upon spectral slopes and ratios (Helms et al., 2008; Spencer et al., 2012). As such, UV–visible spectroscopy has been shown to be effective for determining DOC concentrations in temperate freshwater systems (De Haan et al., 1982; Tipping et al., 2009; Carter et al., 2012; Peacock et al., 2014; Causse et al., 2016) as well as tropical catchments (Yamashita et al., 2010; Pereira et al., 2014). Spectrophotometric absorbance over a wide range of wavelengths has been used as a proxy for DOC, ranging from 250 nm (De Haan et al., 1982) to 562 nm (Carpenter and Smith,

* Corresponding author. Department of Geography, 1st Floor, Bennett Building, University of Leicester, Leicester, LE1 7RH, UK.
E-mail address: sc606@le.ac.uk (S. Cook).

http://dx.doi.org/10.1016/j.watres.2017.02.059

1984). Peacock et al. (2014) investigated the effectiveness of a range of single wavelengths between 230 and 800 nm as a proxy for DOC in waters draining two temperate upland catchments in the UK. The strongest correlations between absorbance and DOC were at 230 nm, 254 nm and 263 nm (Peacock et al., 2014). The correlation between absorbance and DOC was observed to decline with increasing wavelength, a finding also noted by Asmala et al. (2012) and Grayson and Holden (2016).

A further spectrophotometric approach is to use an empirical model based on two or more wavelengths to calculate DOC concentrations (e.g. 270 nm and 350 nm; Tipping et al., 2009; Carter et al., 2012). This proxy technique is based on the ratio of optical absorbance of a DOC molecule at a given wavelength (nm) to DOC, referred to as the extinction coefficient (E; units l g^{-1} cm^{-1}; Tipping et al., 2009) otherwise known as SUVA (specific UV absorbance). Developing this further Tipping et al. (2009) describe a two-component model that can predict DOC based on the linear sum of two components A and B (Carter et al., 2012). Both components have different features giving them distinct spectra; component A absorbs UV light strongly whereas component B absorbs it weakly (Carter et al., 2012). The model uses these optical absorbance properties as well as differing E coefficients, at two different wavelengths, to estimate DOC concentrations using a number of steps (Carter et al., 2012). A more detailed description of the model and parametrization, as outlined by Carter et al. (2012), is presented in Section 2.2.

A set of universal extinction coefficients (EA λ_1; EA λ_2; EB λ_1; EB λ_2) for the model, at wavelengths 270 and 350 nm, were generated by Carter et al. (2012) using a large number (n = 1700) of surface water samples collected from the UK and Canada. In principle, any pair of wavelengths can be used (Carter et al., 2012) but 270 and 350 nm have been found to provide particularly robust DOC estimations. For a higher degree of accuracy the universal extinction coefficients can be adjusted for individual sites to produce a calibrated dataset. Carter et al. (2012) found that their two-wavelength method improved the fit between modelled and measured DOC concentrations compared to a single wavelength approach. The practicality and wide applicability of this two-wavelength approach has also been demonstrated by Peacock et al. (2014) who used the universal parameters to measure DOC in surface water, but found that the model had to be re-parameterised to calculate DOC in pore water. It would be useful if the same parameterization could be used to calculate DOC concentrations for other systems, including samples from tropical peatlands. Due to the differing environmental conditions and peat chemistry experienced between temperate and tropical regions, the composition of DOC from these systems is likely to vary. It is, therefore, important that these models are validated on tropical samples, particularly given the increased interest in tropical peat dynamics in recent years.

At present we are unaware of any studies in the literature that have investigated the suitability of UV–vis spectroscopy methods for measuring DOC concentrations in water samples from tropical peatland catchments and, specifically, from oil palm plantations. While other research has explored tropical DOC concentrations and composition using this method (Johnson et al., 2006; Waterloo et al., 2006; Spencer et al., 2010; Yamashita et al., 2010; Pereira et al., 2014), previous studies have focused on mineral soil-dominated forest catchments, within the Congo (Spencer et al., 2010), Guiana Shield (Yamashita et al., 2010; Pereira et al., 2014) and Amazon basin (Johnson et al., 2006; Waterloo et al., 2006), with only one referencing the presence of peat within their study site (Yamashita et al., 2010). In addition, of these studies only one (Pereira et al., 2014) has applied the original Carter et al. (2012) model in the context of a tropical catchment. In view of the potentially wide applicability of this method, the cost-saving benefits and its potential to produce accurate results without the need for specialised laboratory facilities (particularly valuable for sample analyses at remote field sites), it is important to properly evaluate it. The aims of this investigation are, therefore, three-fold:

1) To investigate the suitability of different wavelength absorbance proxies for tropical DOC determination;
2) To develop a calibration dataset and a set of parameters that can be used to calculate tropical DOC concentrations indirectly;
3) To provide guidance for other tropical researchers on the best UV–vis spectrophotometric approaches to take when analyzing similar samples.

2. Methods

2.1. Site descriptions and sampling

Water samples for this investigation were collected from the Sebungan and Sabaju oil palm estates, located in the Malaysian province of Sarawak, northern Borneo (between 3°07.81′ N and 3°14.91′N and 113°18.72′ E and 113°32.19′E; Fig. 1). Both estates are established on tropical peat soils and cover a collective area of nearly 10,000 ha. Air temperatures within this region are high (mean 26 °C) and there is heavy rainfall throughout the year (~3000 mm received annually: Melling et al., 2005).

Water samples were collected during two field campaigns: (A) 18th to 30th April 2015 and (B) 3rd August to 6th October 2015. All samples were collected in 60 ml Nalgene® bottles and filtered through 0.45 μm cellulose nitrate membrane filters, using a hand-held vacuum pump within 24 h of collection. As there was no spectrophotometer present on site during Campaign A filtered samples were subsequently stored in a fridge at 4 °C for 6–12 weeks, until shipment back to the UK for analysis. However, an onsite Cole-Parmer UV/visible spectrophotometer was present during Campaign B allowing immediate sample analysis. All samples, regardless of campaign, were subjected to cold storage which has been shown to ensure reasonable preservation of DOC between sampling and analysis (Cook et al., 2016). Subsequently, significant alterations to DOC concentrations and spectrophotometric properties would not be expected in between sampling and DOC analysis back in to the UK.

Upon return to the UK, samples collected during Campaign A were analysed in June 2015 and those from Campaign B in November 2015 on a Total Organic Carbon (TOC; Shimadzu) analyser (precision ~ 2–5%; Graneli et al., 1996; Bjorkvald et al., 2008; Shafer et al., 2010) as non-purgeable organic carbon (NPOC), to generate measured DOC concentrations. Prior to analysis, samples were acidified (pH < 3) and sparged with purified air to remove inorganic carbon. Measured DOC concentrations were subsequently calculated using a calibration curve ranging from 0 to 100 mg L^{-1}. Additional standards with concentrations close to those expected in the samples were analysed to check for drift. In parallel, samples were also analysed on a Helios Gamma spectrophotometer to measure UV–vis absorbance at different wavelengths. A set of filtered blanks were analysed in the same manner as the water samples to ensure the suitability of the cellulose nitrate filters for SUVA analysis. Filters leached 0.008 absorbance at 254 nm, and 0.4 mg L^{-1} DOC. However, considering the relatively high DOC concentrations and absorbance values for the majority of water samples, along with the precision of the TOC analyser, leaching was considered negligible.

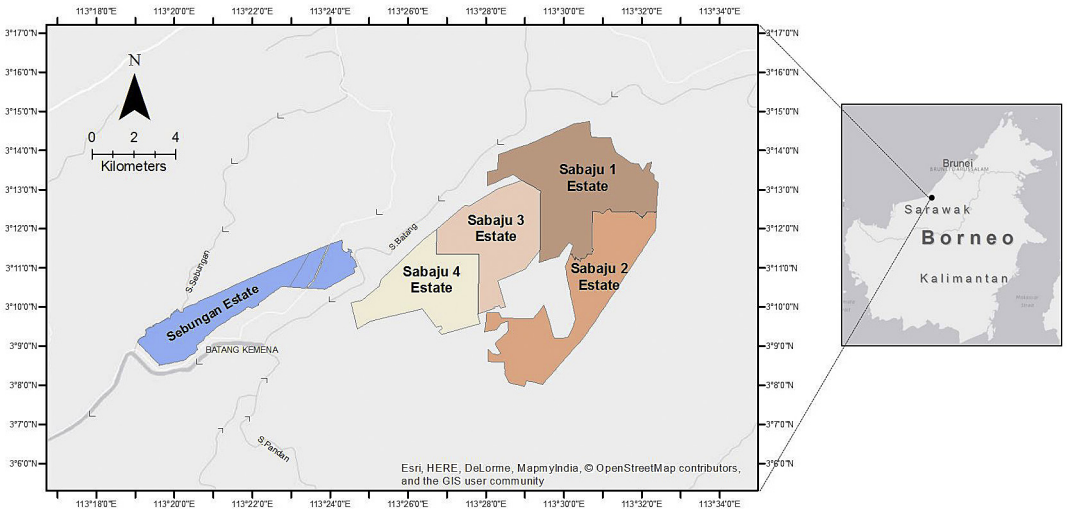

Fig. 1. Location of the Sebungan and Sabaju oil palm estates in Sebauh Bintulu district Sarawak. The estates are bordered by a network of rivers (grey and white lines) namely the Batang Kemena, S. Sebungan, S. Batang and S. Pandan. Arrows indicate direction of water flow.

2.2. Two-wavelength model description

The two wavelength model predicts DOC concentrations (C_{DOC}) on the basis of light absorption at two wavelengths (Tipping et al., 2009; Carter et al., 2012). Briefly,

$$C_{DOC} = \frac{(\alpha_{270} - \alpha_{700})}{E_{270}} + C_{NAC} \quad (1)$$

where α_{270} is the absorbance at 270 nm, α_{700} is the absorbance at 700 nm (used to account for instrumental drift, after Hernes et al., 2008), C_{NAC} is a constant concentration of DOC which does not absorb light (assumed here to be the same as the value reported by Carter et al., 2012 i.e. 0.8 mg L^{-1}) and E_{270} is an extinction coefficient (absorbance cm^{-1} C_{DOC}^{-1}) of the light-absorbing DOC, given by

$$E_{270} = (f_A \cdot E_{A,270}) + (f_B \cdot E_{B,270}) = (f_A \cdot E_{A,270}) + ((1 - f_A) \cdot E_{B,270}) \quad (2)$$

where f_A and f_B are fractions of two components of DOC (A and B: each assumed to have different fixed absorbance spectra) and $E_{A,270}$ and $E_{B,270}$ are, respectively, empirically fitted extinction coefficients for components A and B at 270 nm. The fraction f_A is given by

$$f_A = \frac{E_{B,270} - (R \cdot E_{B,350})}{(R \cdot E_{A,350}) - (R \cdot E_{B,350}) - E_{A,270} + E_{B,270}} \quad (3)$$

in which $E_{A,350}$ and $E_{B,350}$ are, respectively, empirically fitted extinction coefficients for components A and B at 350 nm and R is the measured absorbance ratio at 270 and 350 nm ($\alpha_{270}/\alpha_{350}$). There are four empirically fitted extinction coefficients: $E_{A,270}$, $E_{B,270}$, $E_{A,350}$ and $E_{B,350}$ but only $E_{A,270}$ and $E_{B,270}$ were adjusted in our calibration with $E_{A,350}$ and $E_{B,350}$ unchanged from those reported by Carter et al. (2012).

2.3. Single-wavelength proxy assessment

The performance of a single wavelength (1λ) model for DOC was assessed using non-linear regression between absorbance at individual wavelengths (270 or 350 nm) and measured DOC concentrations in the samples collected in Campaign A. The resulting regression equations were then validated using the samples collected in Campaign B.

2.4. Two-wavelength proxy assessment

Absorbance data (at 270 and 350 nm) were combined with the measured DOC concentrations to generate a calibration data set for the two-wavelength model (2λ: Tipping et al., 2009; Carter et al., 2012). Model parameters (extinction coefficients at each wavelength) were adjusted by trial and error so as to maximize the R^2 value and minimize the sum of squared residuals between absorbance-derived DOC concentration and DOC concentrations measured by the TOC analyser. The calibrated extinction coefficients are displayed in Table 1 alongside the universal extinction coefficients proposed by Carter et al. (2012).

The empirical model was tested on an independent validation data set (water samples collected during Campaign B). These samples were analysed immediately after filtration (to minimize storage losses of DOC) on a Cole-Parmer UV/visible spectrophotometer, in Malaysia, at wavelengths of 270 nm and 350 nm. These UV–vis absorbance values were subsequently used in the calibrated model to calculate DOC concentrations. DOC concentrations were measured on a TOC analyser, using the method previously described. As well as the coefficients derived from the calibration using the samples collected during Campaign A, 'universal calibration coefficients' proposed by Carter et al. (2012) were also used to generate DOC concentrations (Table 1). This allowed the general validity of the universal coefficients in the 2λ model to be evaluated. It should also be noted that a subset of five of the DOC water samples were chosen to cross-check for consistency between the absorbances produced on the UK-based and Malaysian-based spectrophotometers. This comparison showed an average difference in absorbance values of only 0.003 ± 0.004 cm^{-1}.

2.5. Comparisons between approaches

In summary, a total of four approaches were used to estimate DOC concentrations using UV–vis spectrophotometry:

1) 1λ approach using absorbance values at 270 nm ($1\lambda_{270}$)
2) 1λ approach using absorbance values at 350 nm ($1\lambda_{350}$)
3) 2λ approach calibrated on the April 2015 dataset/ Campaign A ($2\lambda_{calibrated}$)

Table 1
Values of the extinction coefficients used by Carter et al. (2012) and those generated from the calibrated data set, where λ1 = 270 nm and λ2 = 350 nm.

Extinction Coefficients	Universal extinction coefficients (L g^{-1})	Calibrated extinction coefficients (L g^{-1})
EA $_{\lambda 1}$	69.3	74.32
EA $_{\lambda 2}$	30	30
EB $_{\lambda 1}$	15.4	15
EB $_{\lambda 2}$	0	0

4) 2λ approach using the 'universal calibration coefficients' (Carter et al., 2012) ($2\lambda_{non\text{-}calibrated}$)

The performance of the four models was assessed using the following metrics:

a) Actual differences between measured and estimated DOC concentrations (mg l^{-1});
b) The coefficient of determination (R^2) for the regression between measured and modelled DOC concentrations;
c) The root mean squared error (RMSE);
d) The Nash-Sutcliffe efficiency (Nash and Sutcliffe, 1970) which is a measure of goodness of fit between the modelled and actual DOC concentrations i.e.:

$$NSE = 1 - \frac{\sum (C_{meas} - C_{est})^2}{\sum \left(C_{meas} - \overline{C_{mean}}\right)^2} \quad (4)$$

where C_{meas} is the measured DOC concentration (TOC analyser), C_{est} is the DOC concentration estimated using the various wavelength proxies and C_{mean} is the mean measured DOC concentration. The closer the NSE is to +1 the stronger the model fit. A value of 0 or lower indicates that the model performs no better than the mean of the data (Nash and Sutcliffe, 1970).

2.6. Statistical analyses

Quantitative data analysis was performed using parametric statistical tests when appropriate (GraphPad Prism, version 6; Microsoft Excel 2013). Normality was tested using the Shapiro-Wilk test.

3. Results

3.1. Single-wavelength approach

3.1.1. Single wavelength model development

Fig. 2 shows the results of a series of regression analyses of modelled and measured DOC concentrations using a single wavelength proxy approach. Measured DOC concentrations for Campaign A data are plotted against modelled DOC concentration using absorbance at 270 nm (Fig. 2a; $1\lambda_{original\text{-}270}$ model) and 350 nm (Fig. 2b; $1\lambda_{original\text{-}350}$ model). Mean pH and electrical conductivity were 3.3 and 173 μS cm^{-1}, respectively. The equations generated in Fig. 2a; b were then used to model the DOC concentrations for the August–October data set using absorbance at 270 nm ($1\lambda_{270}$ model) and 350 nm ($1\lambda_{350}$) and then compared to the corresponding measured concentrations (Fig. 2c; d). Goodness of fit metrics between the three models are displayed in Table 3. Measured DOC concentrations ranged between 8.3 and 82.5 mg L^{-1}. Predicted DOC concentrations ranged between 8.1 and 63.0 mg L^{-1} and between 1.0 and 71.4 mg L^{-1}, for the $1\lambda_{270}$ and $1\lambda_{350}$ models, respectively.

3.2. Two-wavelength approach

3.2.1. Two-wavelength model development and validation

Fig. 3 shows the results of several regression analyses of modelled and measured DOC concentrations that were used to calibrate the model and validate it. The original calibration ($2\lambda_{original\text{-}calibrated}$ model: Fig. 3a) displays the measured DOC concentrations for the April 2015 data set against the modelled DOC concentrations, generated by adjusting the extinction coefficients to maximize the goodness of fit. DOC concentrations ranged from 9.3 to 52.0 mg L^{-1} and 9.3–52.8 mg L^{-1} for the measured and modelled techniques, respectively. This calibrated model was then validated by testing it on the independent data set ($2\lambda_{calibrated}$ model: collected during Campaign B), the results of which are displayed in Fig. 2b. The DOC concentrations from the same data set (Campaign B) were then modelled using the universal extinction coefficients suggested by Carter et al. (2012), as shown in Fig. 3c ($2\lambda_{non\text{-}calibrated}$ model). Respective mean pH and electrical conductivity values were 3.7 and 177 μS cm^{-1} for Campaign B samples. Goodness of fit metrics between the three models are displayed in Table 3. Predicted DOC concentrations ranged from 5.5 to 71.7 mg L^{-1} and from 6.7 to 82.8 mg L^{-1} for the $2\lambda_{calibrated}$ and $2\lambda_{non\text{-}calibrated}$ models, respectively. While the DOC concentration ranges within the validation data set (Fig. 3b; c) were greater than those observed for the calibrated data (Fig. 3a), 92% of the validation data (190 samples out of 206 samples) fell within the broad range encompassed by the DOC calibration (0–60 mg L^{-1}). Accordingly, the majority of the DOC concentration data set was represented.

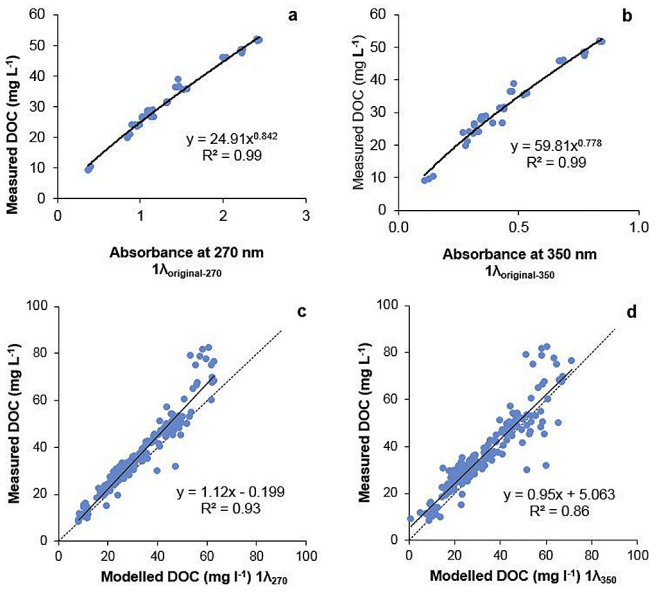

Fig. 2. Regression relationships between measured DOC concentrations from Campaign A and absorbance at 270 nm (a) and 350 nm (b) along with (c) modelled DOC concentrations from Campaign B derived using the equation generated in (a) and (d) equation generated in (b). Dashed lines show 1:1 relationship.

Table 2
Mean concentration and percentage differences between modelled and measured DOC concentrations (mg L^{-1}) for the four different models using the validation data set (collected during Campaign B). Positive and negative values indicate that modelled DOC concentrations overestimate and underestimate measured DOC concentrations, respectively. n = number of samples.

	$2\lambda_{calibrated}$	$2\lambda_{non\text{-}calibrated}$	$1\lambda_{270}$	$1\lambda_{350}$
n	206	206	206	206
Difference between modelled and measured DOC (mg l^{-1})	−4.1 ± 0.4	1.2 ± 0.3	−3.7 ± 0.3	−3.4 ± 0.4
% Difference between modelled and measured DOC	14.4 ± 0.8	9.7 ± 0.8	11.9 ± 0.5	15.5 ± 1.0

Table 3
Summary of goodness of fit metrics for all development and validation models. R^2 values and slope of regression lines between modelled and measured DOC for the model approaches, along with NSE and RMSE values. n = number of samples.

	Model development			Validation data			
	2λ original-calibrated	1λ original-270	1λ original-350	$2\lambda_{calibrated}$	$2\lambda_{non\text{-}calibrated}$	$1\lambda_{270}$	$1\lambda_{350}$
n	46	46	46	206	206	206	206
R^2	0.98	0.98	0.95	0.87	0.92	0.93	0.86
NSE	N/A	N/A	N/A	0.80	0.91	0.86	0.81
RMSE	1.45	1.51	2.27	6.99	4.82	5.81	6.89

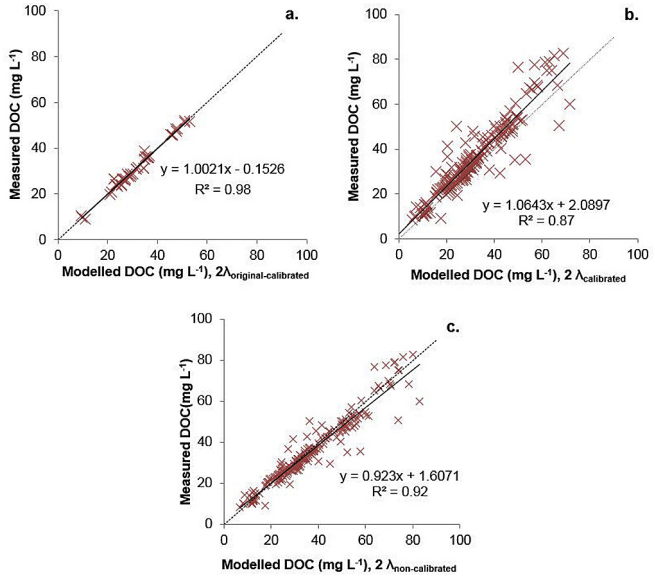

Fig. 3. a) Original model calibration (constructed from April 2015 data/Campaign A). Regression of modelled DOC concentrations (n = 47) against respective measured DOC concentrations. Extinction coefficients were derived independently from the same data used for calibration (calibrated extinction coefficients): $E_{A,\ \lambda1} = 74.32$, $E_{A,\ \lambda2} = 30$, $E_{B,\ \lambda1} = 15$ $E_{B,\ \lambda2} = 0$ **b)** Regression of DOC concentrations from the independent data set ($2\lambda_{calibrated}$ model) (collected from Campaign B), against respective measured DOC concentrations. Model DOC concentrations generated using the calibrated extinction coefficients **c)** Regression of 2 λ modelled DOC concentrations for validation samples against respective measured DOC concentrations using 'universal calibration coefficients' (Carter et al., 2012). Dashed lines show 1:1 relationships.

3.3. Overall assessment of models

The overall effectiveness of the four different models to predict DOC concentrations are summarized in Table 2, displaying the concentration and percentage differences between the modelled and measured DOC. The goodness of fit metrics for all four model approaches are present in Table 3; validation data.

The extinction coefficients for A and B were adjusted to optimize the fit between modelled DOC concentrations and the respective measured values ($R^2 = 0.98$; $p < 0.05$) (Fig. 3 a). Lower and upper 95% confidence intervals were 0.746 and 1.344, respectively. The optimal extinction coefficients for the 2λ model were: $E_{A,270} = 74.32$ L g^{-1}; $E_{A,350} = 30$ L g^{-1}; $E_{B,270} = 15$ L g^{-1}; $E_{B,350} = 0$ L g^{-1}. The $2\lambda_{original\text{-}calibrated}$ model was then tested on an independent validation data set ($2\lambda_{calibrated}$) (Fig. 3 b). The model fit was strong ($R^2 = 0.87$; $p < 0.05$, RMSE = 6.99 mg L^{-1}: Table 3). In general, the calibrated model ($2\lambda_{calibrated}$) tended to underestimate concentrations although on average the mean difference between the modelled and measured values was small (- 4.1 ± 0.4 mg L^{-1}: Table 2). The lower and upper 95% confidence intervals were - 3.3 and - 4.9 mg L^{-1}, respectively. The model fit was also strong using the universal extinction coefficients ($2\lambda_{non\text{-}calibrated}$) cited in Carter et al. (2012) ($R^2 = 0.92$; $p < 0.05$) (Fig. 3 c) with a slightly lower RMSE (4.82 mg L^{-1}). However, this model tended to overestimate DOC concentrations by an average of 1.2 ± 0.3 mg L^{-1} (Fig. 3). 95% confidence intervals were 1.85 (lower) and 0.57 (upper).

Linear regressions between absorbance at single wavelengths and measured DOC concentrations are shown in Fig. 2 (a, b).

Modelled DOC concentrations derived using absorbance at 270 nm were a better fit to measured DOC concentrations ($R^2 = 0.93$; $p < 0.05$: Fig. 2c) than those derived at 350 nm ($R^2 = 0.86$; $p < 0.05$: Fig. 2 d). However, both models tended to underestimate DOC concentrations with mean differences between measured and modelled values ranging from - 3.7 ± 0.3 mg L^{-1} to - 3.4 ± 0.4 mg lL^{-1} for the 270 nm and 350 nm models, respectively (Table 2). Confidence intervals at 95% ranged from − 4.22 to − 4.34 (lower) and − 2.57 to − 3.11 (upper) for the 350 nm and 270 nm models, respectively. Both single wavelength models displayed a threshold-like behaviour between modelled and measured DOC concentrations (Fig. 2 c; d). At approximately 60 mg L^{-1} there appears to be a clear decoupling of the absorbance measurements from the measured DOC data, resulting in the majority of modelled DOC concentrations being underestimated (Fig. 2 c; d). This could be consistent with findings made by Pereira et al. (2014) and therefore supports their concept of the presence of an "invisible" dissolved organic matter (iDOM) component. This non-humic and, therefore, non-chromophoric constituent is undetectable using conventional spectrophotometric methods yet does contribute to the overall DOC pool (Pereira et al., 2014).

The overall statistical performance of all four models was strong (Table 3). The $2\lambda_{non\text{-}calibrated}$ model performed best in terms of NSE and RMSE (respective values 0.91 and 4.82 mg L^{-1}). This was closely followed by the $1\lambda_{270}$ model, which had a slightly higher R^2 value (0.93) but lower NSE and RMSE (respective values 0.86 and 5.81 mg L^{-1}). Relative differences (measured - modelled) between the modelled and measured DOC concentrations across all four

models ranged from 9.7% to 15.5% (Table 2), with the $2\lambda_{non\text{-}calibrated}$ approach producing the smallest % difference. This trend was also observed for the mean absolute differences (modelled − measured) in DOC concentration (Table 2). The highest NSE was produced by the $2\lambda_{non\text{-}calibrated}$ approach (NSE 0.91). The $2\lambda_{calibrated}$ approach produced the lowest NSE (0.80). The intercept of the 270 nm proxy ($1\lambda_{270}$) model was closest to zero (0.20 ± 0.74 mg L^{-1}, $p > 0.05$) and the intercept of the 350 nm proxy ($1\lambda_{350}$) was furthest away from zero (5.06 ± 1.04 mg L^{-1}, $p < 0.05$). However, the slope of the $1\lambda_{350}$ regression was closest to unity (0.95 ± 0.03 mg L^{-1}, $p < 0.0001$) and that of the $1\lambda_{270}$ regression was furthest away from 1 (1.12 ± 0.02 mg L^{-1}, $p < 0.0001$). Of the 2λ approaches, the $2\lambda_{non\text{-}calibrated}$ model had a closer intercept to zero (1.61 ± 0.77 mg L^{-1}, $p < 0.05$) than the $2\lambda_{calibrated}$ model (2.09 ± 0.97 mg L^{-1}, $p < 0.05$) and also had a slope which was closer to unity (0.92 ± 0.02 mg L^{-1}, $p < 0.0001$).

4. Discussion

All four models performed well statistically suggesting that tropical DOC concentrations in surface waters can be estimated accurately using UV–vis spectroscopy. Both the two-wavelength and single-wavelength approaches exhibited similar statistical performance and were both suitable as DOC concentration proxies, reinforcing findings reported for temperate peatland waters by Peacock et al. (2014).

Carter et al. (2012) found that a two-wavelength model improved R^2 values by 0.02 and 0.05 compared to 270 and 350 nm UV proxies, respectively. However, our data suggest that the single-wavelength model at 270 nm produced the strongest R^2 value and the second highest NSE, suggesting that it is as robust as a two-wavelength proxy. This is in agreement with other previous studies (Asmala et al., 2012; Peacock et al., 2013, 2014) and is explained by both the higher resolution given by a shorter wavelength i.e. for which optical absorbance is observed to decrease with increasing wavelength (Wang and Hsieh, 2001) and the fact that peatland DOC is largely composed of aromatic humic substances that strongly absorb light in the UV range (Khan et al., 2014; Thurman, 1985). However, the slope of the regression between modelled and measured DOC concentrations was furthest from unity for the $1\lambda_{270}$ model.

Interestingly (and somewhat surprisingly), the universal $2\lambda_{non\text{-}calibrated}$ model (Carter et al., 2012) outperformed the $2\lambda_{calibrated}$ model in terms of NSE and mean difference between modelled and measured DOC concentrations for the validation dataset. The universal calibration parameters cited by Carter et al. (2012) were generated using a large number of samples (n = 1700) from high-latitude peatlands collected over a range of different seasons. Consequently, the range of environmental conditions captured by the universal calibration data set and the number of samples collected was higher than the calibration data set employed here and may help to explain this finding, despite the fact that the data used by Carter et al. (2012) were derived from a different climate zone. In addition, our calibration data were collected in April which is at the tail end of the wet season in Sarawak, whereas the data used for validation (August to October) were collected at the end of the dry season. Seasonal variations in both the quantity and quality of DOC have been observed in other studies (e.g. Peacock et al., 2014) and may also explain why a wet-season-calibration did not represent dry-season DOC as well as expected. This is further reinforced by both Johnson et al. (2006) and Pereira et al. (2014) who noted distinct seasonal differences in the composition of tropical DOC. In addition, data used to derive the original calibrated model (Campaign A) were applied to a data set analysed much more rapidly after collection (Campaign B). Therefore, some of the overestimations made by the $2\lambda_{calibrated}$ model could be due to small DOC losses during storage, although an independent assessment of such cold storage losses suggested that they are modest (Cook et al., 2016). As such, this offers further opportunities to improve upon our existing model and the locally-calibrated model may be improved as sampling continues.

The performance of the universal calibration coefficients (Carter et al., 2012) in this tropical surface water system is encouraging. From a practical perspective, this suggests that other tropical researchers may also be able to use these parameters, in the absence of their own calibration data set. This would allow DOC concentrations to be determined soon after sampling without having to ship samples from remote field locations to the laboratory for site-specific calibrations (although this is always the preferred practice).

There will always be a need for quality control checks on proxy DOC determinations, but the fact that UV–vis spectroscopy is able to predict tropical DOC concentrations accurately and rapidly is extremely promising because it offers the ability to generate *in-situ* data which may improve both the spatial and temporal range of DOC measurements. This may be particularly important for research groups working in remote locations which lack immediate access to specialised (and often expensive), analytical equipment. DOC concentrations and quality (absorbance and fluorescence properties) can change in stored water samples over time even after acidification and or freezing (Spencer et al., 2007; Fellman et al., 2008; Peacock et al., 2015; Cook et al., 2016), so the possibility of immediate post-collection analysis is attractive.

5. Conclusions

The concentrations of DOC in tropical water samples collected from peat-dominated catchments can be determined accurately using both single- and two-wavelength spectrophotometric techniques. This offers researchers the potential to analyse samples rapidly post-collection using an inexpensive method and could be invaluable when working in remote tropical field sites.

Acknowledgements

We thank the Malaysian Oil Palm Board (grant: R010913000); the University of Aberdeen, the University of St. Andrews, and Sarawak Oil Palms Berhad; and the Natural Environment Research Council (NERC) (grant: X402NE53) for financial support. V.G and S.C are grateful for support from the AXA Research Fund. S.E.P and M.J.W are grateful to the University of Leicester for study leave. S.C performed the Malaysian field data collection, facilitated by the field supported provided by K.L.K. S.C and M.P analysed and interpreted the data. All authors discussed the results and commented on the manuscript. We also wish to thank two anonymous reviewers for their helpful comments that helped to improve the manuscript.

References

Abrams, J.F., Hohn, S., Rixen, T., Baum, A., Merico, A., 2015. The impact of Indonesian peatland degradation on downstream marine ecosystems and the global carbon cycle. Glob. Chang. Biol. 22, 325–337.
Asmala, E., Stedmon, C.A., Thomas, D.N., 2012. Linking CDOM spectral absorption to dissolved organic carbon concentrations and loadings in boreal estuaries. Estuar. Coast. Shelf Sci. 111, 107–117.
Bjorkvald, L., Buffan, I., Laudon, H., Morth, C.-M., 2008. Geochim. Cosmochim. Acta 72, 2789–2804.
Carpenter, P.D., Smith, J.D., 1984. Simultaneous spectrophotometric determination of humic acid and iron in water. Anal. Chim. Acta 159, 299–308.
Carter, H.T., Tipping, E., Kopriyniak, J.-F., Miller, M.P., Cookson, B., Hamilton-Taylor, J., 2012. Freshwater DOM quantity and quality from a two-component model of UV absorbance. Water Res. 46, 4532–4542.
Causse, J., Thomas, O., Jung, A.-V., Thomas, M.-F., 2016. Direct DOC and nitrate

determination in water using dual pathlength and second derivative UV spectrophotometry. Water Res. 108, 312–319.
Clark, J.M., Bottrell, S.H., Evans, C.D., Monteith, D.T., Bartlett, R., Rose, R., Newton, J.R., Chapman, P.J., 2010. The importance of the relationship between scale and process in understanding long-term DOC dynamics. Sci. Total Environ. 408, 2768–2775.
Cole, J.J., Prairie, Y.T., Caraco, N.F., McDowell, W.H., Tranvik, L.J., Striegl, R.G., Duarte, C.M., Kortelainen, P., Downing, J.A., Middelbugh, J.J., Melack, J., 2007. Plumbing the global carbon cycle: integrating inland waters into the terrestrial carbon budget. Ecosystems 10, 172–185.
Cook, S., Peacock, M., Evans, C.D., Page, S.E., Whelan, M., Gauci, V., Khoon, K.L., 2016. Cold Storage as a method for the long-term preservation of tropical dissolved organic carbon (DOC). Mires Peat 18, 1–8.
De Haan, H., De Boer, T., Kramer, H.,A., Voerman, J., 1982. Applicability of light absorbance as a measure of organic carbon in humic lake water. Water Resour. 16, 1047–1050.
Evans, C.D., Jones, T.G., Burden, A., Ostle, N., Piotr, Z., Cooper, M.D.A., Peacock, M., Clark, J.M., Oulehle, F., Cooper, D., Freeman, C., 2012. Acidity controls on dissolved organic carbon mobility in organic soils. Glob. Chang. Biol. 18, 3317–3331.
Evans, C.D., Page, S.E., Jones, T., Moore, S., Gauci, V., Laiho, R., Hruška, J., Allott, T.E.H., Billett, M.F., Tipping, E., Freeman, C., Garnett, M.H., 2014. Contrasting vulnerability of drained tropical and high-latitude peatlands to fluvial loss of stored carbon. Biogeochem. Cycles 28, 1215–1234.
Fellman, J.B., D'Amore, D.V., Hood, E., 2008. An evaluation of freezing as a preservation technique for analyzing dissolved organic C, N and P in surface water samples. Sci. Total Environ. 392, 305–312.
Fellman, J.B., Spencer, R.G.M., Raymond, P.A., Pettit, N.E., Skrzypek, G., Hernes, P.J., Grierson, P.F., 2014. Dissolved organic carbon biolability decreases along with its modernization in fluvial networks in an ancient landscape. Ecology 95, 2622–2632.
Graneli, W., Lindell, M., Tranvik, L., 1996. Photo-oxidative production of dissolved inorganic carbon in lakes of different humic content. Limnol. Oceanogr. 41, 698–706.
Grayson, R.P., Holden, J., 2016. Improved automation of dissolved organic carbon sampling for organic-rich surface waters. Sci. Total Environ. 543, 44–51.
Helms, J.R., Stubbins, A., Ritchie, J.D., Minor, E.C., 2008. Absorption spectral slopes and slope ratios as indicators of molecular weight, source, and photobleaching of chromophoric dissolved organic matter. Limnol. Oceanogr. 53, 955–969.
Hernes, P.J., Spencer, R.G.M., Dyda, R.Y., Pellerin, B.A., Bachand, P.A.M., Bergamaschi, A., 2008. The role of hydrologic regimes on dissolved organic carbon composition in an agricultural watershed. Geochim. Cosmochim. Acta 72, 5266–5277.
Hulatt, C.J., Kaartokallio, H., Oinonen, M., Sonninen, E., Stedmon, C.A., Thomas, D.N., 2014. Radiocarbon dating of fluvial organic matter reveals land-use impacts in boreal peatlands. Environ. Sci. Technol. 48, 12543–12551.
Johnson, M.S., Lehmann, J., Couto, E.G., Filho, J.P.N., Riha, S.J., 2006. DOC and DIC in flowpaths of Amazonian headwater catchments with hydrologically contrasting soils. Biogeochemistry 81, 45–57.
Khan, S., Yaoguo, W., Xiaoyan, Z., Youning, X., Jianghua, Z., Sihai, 2014. Estimation of concentration of dissolved organic matter from sediment by using UV-visible spectrophotometer. Int. J. Environ. Pollut. Remediat. 2, 24–29.
Melling, L., Hatano, R., Goh, K.J., 2005. Soil CO2 flux from three ecosystems in tropical peatland of Sarawak, Malaysia. Tellus 75, 1–11.
Moore, S., Evans, C.D., Page, S.E., Garnett, M.H., Jones, T.H., Freeman, C., Hooijer, A., Wiltshire, A., Limin, S., Gauci, V., 2013. Deep instability of deforested tropical peatlands revealed by fluvial organic carbon fluxes. Nature 493, 660–664.
Moore, S., Gauci, V., Evans, C.D., Page, S.E., 2011. Fluvial organic carbon losses from a Bornean blackwater river. Biogeosciences 8, 901–909.
Muller, D., Warneke, T., Rixen, T., Muler, M., Mujahids, A., Banges, H.W., Notholt, J., 2015. Fate of peat-derived carbon and associated CO2 and CO emissions from two Southeast Asian estuaries. Biogeosciences Discuss. 12, 8299–8340.
Nash, J.E., Sutcliffe, J.V., 1970. River flow forecasting through conceptual models part I–a discussion of principles. J. Hydrol. 10, 282–290.
Peacock, M., Burden, A., Cooper, M., Dunn, C., Evans, C.D., Fenner, N., Freeman, C., Gough, R., Hughes, D., Jones, T., Lebron, I., West, M., Zielinski, P., 2013. Quantifying dissolved organic carbon concentrations in upland catchments using phenolic proxy measurements. J. Hydrol. 477, 251–260.
Peacock, M., Evans, C.D., Fenner, N., Freeman, C., Gough, R., Jones, T.G., Lebron, I., 2014. UV-visible absorbance spectroscopy as a proxy for peatland dissolved organic carbon (DOC) quantity and quality: considerations on wavelength and absorbance degradation. Environ. Sci. Process. Impacts 16, 1445–1461.
Peacock, M., Freeman, C., Gauci, V., Lebron, I., Evans, C.D., 2015. Investigations of freezing and cold storage for the analysis of peatland dissolved organic carbon (DOC) and absorbance properties. Environ. Sci. Process. Impacts 17, 1290–1301.
Pereira, R., Bovolo, C.I., Spencer, R.G.M., Hernes, P.J., Tipping, E., Vieth-Hillebrand, A., Pedentchouk, N., Chappell, N.A., Parkin, G., Wagner, 2014. Mobilization of optically invisible dissolved organic matter in response to rainstorm events in a tropical forest headwater river. Geophys. Res. Lett. 41, 1202–1208.
Peuravuori, J., Pihlaja, K., 1997. Molecular size distribution and spectroscopic properties of aquatic humic substances. Anal. Chim. Acta 337, 133–149.
Rixen, T., Baum, A., Wit, F., Samiaji, J., 2016. Carbon leaching from tropical peat soils and consequence for carbon balances. Front. Earth Sci. 4 http://dx.doi.org/10.3389/feart.2016.00074.
Shafer, M.M., Perkins, D.A., Antkiewicz, D.S., Stone, E.A., Qurasishi, T.A., Schauer, J.J., 2010. Reactive oxygen species activity and chemical speciation of size-fractionated atmospheric particulate matter from Lahore, Pakistan: an important role for transition metals. J. Environ. Monit. 12, 704–715.
Spencer, R.G.M., Bolton, L., Baker, A., 2007. Freeze/thaw and pH effects on freshwater dissolved organic matter fluorescence and absorbance properties from a number of UK locations. Water Res. 41, 2941–2950.
Spencer, R.G.M., Hernes, P.J., Ruf, R., Baker, A., Dyda, R.Y., Stubbins, A., Six, J., 2010. Temporal controls on dissolved organic matter and lignin biogeochemistry in a pristine tropical river, Democratic Republic of Congo. J. Geophys. Res. 115 http://dx.doi.org/10.1029/2009JG001180.
Spencer, R.G.M., Butler, K.D., Aiken, G.R., 2012. Dissolved organic carbon and chromophoric dissolved organic matter properties of rivers in the USA. J. Geophys. Res. 117 http://dx.doi.org/10.1029/2011JG001928.
Thurman, E.M., 1985. Developments in biogeochemistry. In: Nijhoff, M. (Ed.), Organic Geochemistry of Natural Waters. Junk Publishers, Dordrecht, Netherlands.
Tipping, E., Corbishley, H.T., Koprivnjak, J.-F., Lapworth, D.J., Miller, M.P., Vincent, C.D., Hamilton-Taylor, J., 2009. Quantification of natural DOM from UV absorption at two wavelengths. Environ. Chem. 6, 472–476.
Wang, G.-S., Hsieh, S.-T., 2001. Monitoring natural organic matter with scanning spectrophotometer. Environ. Int. 26, 205–212.
Waterloo, M.J., Oliveira, S.M., Drucker, D.P., Nobre, A.D., Cuartas, L.A., Hodnett, M.G., Langedijk, I., Jans, W.W.p., Tomasella, J., de Araujo, A.C., Pimentel, T.P., Estrada, J.C.M., 2006. Export of orgnic carbon in run-off from an Amazonian rainforest backwater catchment. Hydrol. Process. 20, 2581–2597.
Weishaar, J.L., Aiken, G.R., Bergamaschi, B.A., Fram, M.S., Fujii, R., Mopper, K., 2003. Evaluation of specific ultraviolet absorbance as an indicator of the chemical composition and reactivity of dissolved organic carbon. Environ. Sci. Technol. 37, 4702–4708.
Yamashita, Y., Maie, N., Briceño, H., Jaffé, R., 2010. Optical characterization of dissolved organic matter in tropical rivers of the Guayana Shield, Venezuela. J. Geophys. Res. 115 http://dx.doi.org/10.1029/2009JG000987.